

World Journal of *Clinical Cases*

World J Clin Cases 2022 June 16; 10(17): 5518-5933



MINIREVIEWS

- 5518 Occult hepatitis B – the result of the host immune response interaction with different genomic expressions of the virus
Gherlan GS
- 5531 Pulmonary complications of portal hypertension: The overlooked decompensation
Craciun R, Mocan T, Procopet B, Nemes A, Tefas C, Sparchez M, Mocan LP, Sparchez Z
- 5541 Ethical review of off-label drugs during the COVID-19 pandemic
Li QY, Lv Y, An ZY, Dai NN, Hong X, Zhang Y, Liang LJ

ORIGINAL ARTICLE**Case Control Study**

- 5551 Gut peptide changes in patients with obstructive jaundice undergoing biliary drainage: A prospective case control study
Pavić T, Pelajić S, Blažević N, Kralj D, Milošević M, Mikolasevic I, Lerotic I, Hrabar D

Retrospective Cohort Study

- 5566 Longitudinal assessment of liver stiffness by transient elastography for chronic hepatitis C patients
Mezina A, Krishnan A, Woreta TA, Rubenstein KB, Watson E, Chen PH, Rodriguez-Watson C

Retrospective Study

- 5577 Clinical evaluation of prone position ventilation in the treatment of acute respiratory distress syndrome induced by sepsis
Xia WH, Yang CL, Chen Z, Ouyang CH, Ouyang GQ, Li QG
- 5586 Three-dimensional arterial spin labeling and diffusion kurtosis imaging in evaluating perfusion and infarct area size in acute cerebral ischemia
Jiang YY, Zhong ZL, Zuo M
- 5595 Intrathecal methotrexate in combination with systemic chemotherapy in glioblastoma patients with leptomeningeal dissemination: A retrospective analysis
Kang X, Chen F, Yang SB, Wang YL, Qian ZH, Li Y, Lin H, Li P, Peng YC, Wang XM, Li WB
- 5606 Hepatic epithelioid hemangioendothelioma: Clinical characteristics, diagnosis, treatment, and prognosis
Zhao M, Yin F
- 5620 Difference between type 2 gastroesophageal varices and isolated fundic varices in clinical profiles and portosystemic collaterals
Song YH, Xiang HY, Si KK, Wang ZH, Zhang Y, Liu C, Xu KS, Li X

- 5634** Assessment of incidental focal colorectal uptake by analysis of fluorine-18 fluorodeoxyglucose positron emission tomography parameters

Lee H, Hwang KH, Kwon KA

Observational Study

- 5646** "Zero ischemia" laparoscopic partial nephrectomy by high-power GreenLight laser enucleation for renal carcinoma: A single-center experience

Zhang XM, Xu JD, Lv JM, Pan XW, Cao JW, Chu J, Cui XG

- 5655** High Eckardt score and previous treatment were associated with poor postperoral endoscopic myotomy pain control: A retrospective study

Chen WN, Xu YL, Zhang XG

- 5667** Higher volume growth rate is associated with development of worrisome features in patients with branch duct-intraductal papillary mucinous neoplasms

Innocenti T, Danti G, Lynch EN, Dragoni G, Gottin M, Fedeli F, Palatresi D, Biagini MR, Milani S, Miele V, Galli A

Prospective Study

- 5680** Application of a new anatomic hook-rod-pedicle screw system in young patients with lumbar spondylolysis: A pilot study

Li DM, Li YC, Jiang W, Peng BG

META-ANALYSIS

- 5690** Systematic review of Yougui pills combined with levothyroxine sodium in the treatment of hypothyroidism

Liu XP, Zhou YN, Tan CE

CASE REPORT

- 5702** Allogeneic stem cell transplantation-A curative treatment for paroxysmal nocturnal hemoglobinuria with PIGT mutation: A case report

Schenone L, Notarantonio AB, Latger-Cannard V, Fremeaux-Bacchi V, De Carvalho-Bittencourt M, Rubio MT, Muller M, D'Aveni M

- 5708** Gray zone lymphoma effectively treated with cyclophosphamide, doxorubicin, vincristine, prednisolone, and rituximab chemotherapy: A case report

Hojo N, Nagasaki M, Mihara Y

- 5717** Diagnosis of spontaneous isolated superior mesenteric artery dissection with ultrasound: A case report

Zhang Y, Zhou JY, Liu J, Bai C

- 5723** Adrenocorticotrophic hormone-secreting pancreatic neuroendocrine carcinoma with multiple organ infections and widespread thrombosis: A case report

Yoshihara A, Nishihama K, Inoue C, Okano Y, Eguchi K, Tanaka S, Maki K, Fridman D'Alessandro V, Takeshita A, Yasuma T, Uemura M, Suzuki T, Gabazza EC, Yano Y

- 5732** Management of the palato-radicular groove with a periodontal regenerative procedure and prosthodontic treatment: A case report

Ling DH, Shi WP, Wang YH, Lai DP, Zhang YZ

- 5741** Combined thoracic paravertebral block and interscalene brachial plexus block for modified radical mastectomy: A case report
Hu ZT, Sun G, Wang ST, Li K
- 5748** Chondromyxoid fibroma of the cervical spine: A case report
Li C, Li S, Hu W
- 5756** Preterm neonate with a large congenital hemangioma on maxillofacial site causing thrombocytopenia and heart failure: A case report
Ren N, Jin CS, Zhao XQ, Gao WH, Gao YX, Wang Y, Zhang YF
- 5764** Simultaneous multiple primary malignancies diagnosed by endoscopic ultrasound-guided fine-needle aspiration: A case report
Yang J, Zeng Y, Zhang JW
- 5770** Neuroendocrine tumour of the descending part of the duodenum complicated with schwannoma: A case report
Zhang L, Zhang C, Feng SY, Ma PP, Zhang S, Wang QQ
- 5776** Massive hemothorax following internal jugular vein catheterization under ultrasound guidance: A case report
Kang H, Cho SY, Suk EH, Ju W, Choi JY
- 5783** Unilateral adrenal tuberculosis whose computed tomography imaging characteristics mimic a malignant tumor: A case report
Liu H, Tang TJ, An ZM, Yu YR
- 5789** Modified membrane fixation technique in a severe continuous horizontal bone defect: A case report
Wang LH, Ruan Y, Zhao WY, Chen JP, Yang F
- 5798** Surgical repair of an emergent giant hepatic aneurysm with an abdominal aortic dissection: A case report
Wen X, Yao ZY, Zhang Q, Wei W, Chen XY, Huang B
- 5805** Heterotopic ossification beneath the upper abdominal incision after radical gastrectomy: Two case reports
Zhang X, Xia PT, Ma YC, Dai Y, Wang YL
- 5810** Non-alcoholic Wernicke encephalopathy in an esophageal cancer patient receiving radiotherapy: A case report
Zhang Y, Wang L, Jiang J, Chen WY
- 5816** New approach for the treatment of vertical root fracture of teeth: A case report and review of literature
Zhong X, Yan P, Fan W
- 5825** Ultrasound-guided microwave ablation as a palliative treatment for mycosis fungoides eyelid involvement: A case report
Chen YW, Yang HZ, Zhao SS, Zhang Z, Chen ZM, Feng HH, An MH, Wang KK, Duan R, Chen BD
- 5833** Pulp revascularization on an adult mandibular right second premolar: A case report
Yang YQ, Wu BL, Zeng JK, Jiang C, Chen M

- 5841** Barrett's esophagus in a patient with bulimia nervosa: A case report
Gouda A, El-Kassas M
- 5846** Spontaneous gallbladder perforation and colon fistula in hypertriglyceridemia-related severe acute pancreatitis: A case report
Wang QP, Chen YJ, Sun MX, Dai JY, Cao J, Xu Q, Zhang GN, Zhang SY
- 5854** Beware of gastric tube in esophagectomy after gastric radiotherapy: A case report
Yurttas C, Wichmann D, Gani C, Bongers MN, Singer S, Thiel C, Koehngrainer A, Thiel K
- 5861** Transition from minimal change disease to focal segmental glomerulosclerosis related to occupational exposure: A case report
Tang L, Cai Z, Wang SX, Zhao WJ
- 5869** Lung adenocarcinoma metastasis to paranasal sinus: A case report
Li WJ, Xue HX, You JQ, Chao CJ
- 5877** Follicular lymphoma presenting like marginal zone lymphoma: A case report
Peng HY, Xiu YJ, Chen WH, Gu QL, Du X
- 5884** Primary renal small cell carcinoma: A case report
Xie K, Li XY, Liao BJ, Wu SC, Chen WM
- 5893** Gitelman syndrome: A case report
Chen SY, Jie N
- 5899** High-frame-rate contrast-enhanced ultrasound findings of liver metastasis of duodenal gastrointestinal stromal tumor: A case report and literature review
Chen JH, Huang Y
- 5910** Tumor-like disorder of the brachial plexus region in a patient with hemophilia: A case report
Guo EQ, Yang XD, Lu HR
- 5916** Response to dacomitinib in advanced non-small-cell lung cancer harboring the rare delE709_T710insD mutation: A case report
Xu F, Xia ML, Pan HY, Pan JW, Shen YH
- 5923** Loss of human epidermal receptor-2 in human epidermal receptor-2+ breast cancer after neoadjuvant treatment: A case report
Yu J, Li NL

LETTER TO THE EDITOR

- 5929** Repetitive transcranial magnetic stimulation for post-traumatic stress disorder: Lights and shadows
Concerto C, Lanza G, Fisticaro F, Pennisi M, Rodolico A, Torrisi G, Bella R, Aguglia E

ABOUT COVER

Editorial Board Member of *World Journal of Clinical Cases*, Raden Andri Primadhi, MD, PhD, Assistant Professor, Surgeon, Department of Orthopaedics and Traumatology, Universitas Padjadjaran Medical School, Hasan Sadikin Hospital, Bandung 40161, Indonesia. randri@unpad.ac.id

AIMS AND SCOPE

The primary aim of *World Journal of Clinical Cases* (*WJCC*, *World J Clin Cases*) is to provide scholars and readers from various fields of clinical medicine with a platform to publish high-quality clinical research articles and communicate their research findings online.

WJCC mainly publishes articles reporting research results and findings obtained in the field of clinical medicine and covering a wide range of topics, including case control studies, retrospective cohort studies, retrospective studies, clinical trials studies, observational studies, prospective studies, randomized controlled trials, randomized clinical trials, systematic reviews, meta-analysis, and case reports.

INDEXING/ABSTRACTING

The *WJCC* is now indexed in Science Citation Index Expanded (also known as SciSearch®), Journal Citation Reports/Science Edition, Scopus, PubMed, and PubMed Central. The 2021 Edition of Journal Citation Reports® cites the 2020 impact factor (IF) for *WJCC* as 1.337; IF without journal self cites: 1.301; 5-year IF: 1.742; Journal Citation Indicator: 0.33; Ranking: 119 among 169 journals in medicine, general and internal; and Quartile category: Q3. The *WJCC*'s CiteScore for 2020 is 0.8 and Scopus CiteScore rank 2020: General Medicine is 493/793.

RESPONSIBLE EDITORS FOR THIS ISSUE

Production Editor: *Hua-Ge Yan*; Production Department Director: *Xiang Li*; Editorial Office Director: *Jim-Lai Wang*.

NAME OF JOURNAL

World Journal of Clinical Cases

ISSN

ISSN 2307-8960 (online)

LAUNCH DATE

April 16, 2013

FREQUENCY

Thrice Monthly

EDITORS-IN-CHIEF

Bao-Gan Peng, Jerzy Tadeusz Chudek, George Kontogeorgos, Maurizio Serati, Ja Hyeon Ku

EDITORIAL BOARD MEMBERS

<https://www.wjgnet.com/2307-8960/editorialboard.htm>

PUBLICATION DATE

June 16, 2022

COPYRIGHT

© 2022 Baishideng Publishing Group Inc

INSTRUCTIONS TO AUTHORS

<https://www.wjgnet.com/bpg/gerinfo/204>

GUIDELINES FOR ETHICS DOCUMENTS

<https://www.wjgnet.com/bpg/GerInfo/287>

GUIDELINES FOR NON-NATIVE SPEAKERS OF ENGLISH

<https://www.wjgnet.com/bpg/gerinfo/240>

PUBLICATION ETHICS

<https://www.wjgnet.com/bpg/GerInfo/288>

PUBLICATION MISCONDUCT

<https://www.wjgnet.com/bpg/gerinfo/208>

ARTICLE PROCESSING CHARGE

<https://www.wjgnet.com/bpg/gerinfo/242>

STEPS FOR SUBMITTING MANUSCRIPTS

<https://www.wjgnet.com/bpg/GerInfo/239>

ONLINE SUBMISSION

<https://www.f6publishing.com>

Retrospective Study

Three-dimensional arterial spin labeling and diffusion kurtosis imaging in evaluating perfusion and infarct area size in acute cerebral ischemia

Yan-Yan Jiang, Zhi-Lin Zhong, Min Zuo

Specialty type: Radiology, nuclear medicine and medical imaging**Provenance and peer review:** Unsolicited article; Externally peer reviewed.**Peer-review model:** Single blind**Peer-review report's scientific quality classification**Grade A (Excellent): 0
Grade B (Very good): B
Grade C (Good): C
Grade D (Fair): 0
Grade E (Poor): 0**P-Reviewer:** Cvijic M, Slovenia;
Narain R, Canada**Received:** January 6, 2022**Peer-review started:** January 6, 2022**First decision:** February 14, 2022**Revised:** March 1, 2022**Accepted:** April 9, 2022**Article in press:** April 9, 2022**Published online:** June 16, 2022**Yan-Yan Jiang**, Department of Magnetic Resonance, Wuhan Asia General Hospital, Wuhan 430056, Hubei Province, China**Zhi-Lin Zhong**, Department of Radiology, Wuhan Yaxin General Hospital, Wuhan 430056, Hubei Province, China**Min Zuo**, Department of Radiology, Wuhan Hanyang Hospital, Wuhan University of Science and Technology, Wuhan 430050, Hubei Province, China**Corresponding author:** Min Zuo, BM BCh, Associate Chief Physician, Department of Radiology, Wuhan Hanyang Hospital, Wuhan University of Science and Technology, No. 53 Moohu Road, Anyang District, Wuhan 430050, Hubei Province, China. ypzm0518@163.com

Abstract

BACKGROUND

Early thrombolytic therapy is crucial to treat acute cerebral infarction, especially since the onset of thrombolytic therapy takes 1-6 h. Therefore, early diagnosis and evaluation of cerebral infarction is important.

AIM

To investigate the diagnostic value of magnetic resonance multi-delay three-dimensional arterial spin labeling (3DASL) and diffusion kurtosis imaging (DKI) in evaluating the perfusion and infarct area size in patients with acute cerebral ischemia.

METHODS

Eighty-four patients who experienced acute cerebral ischemia from March 2019 to February 2021 were included. All patients in the acute stage underwent magnetic resonance-based examination, and the data were processed by the system's own software. The apparent diffusion coefficient (ADC), average diffusion coefficient (MD), axial diffusion (AD), radial diffusion (RD), average kurtosis (MK), radial kurtosis (fairly RK), axial kurtosis (AK), and perfusion parameters post-labeling delays (PLD) in the focal area and its corresponding area were compared. The correlation between the lesion area of cerebral infarction under MK and MD and T2-weighted imaging (T2WI) was analyzed.

RESULTS

The DKI parameters of focal and control areas in the study subjects were compared. The ADC, MD, AD, and RD values in the lesion area were significantly lower than those in the control area. The MK, RK, and AK values in the lesion area were significantly higher than those in the control area. The MK/MD value in the infarct lesions was used to determine the matching situation. MK/MD < 5 mm was considered matching and MK/MD ≥ 5 mm was considered mismatching. PLD1.5s and PLD2.5s perfusion parameters in the central, peripheral, and control areas of the infarct lesions in MK/MD-matched and -unmatched patients were not significantly different. PLD1.5s and PLD2.5s perfusion parameter values in the central area of the infarct lesions in MK/MD-matched and -unmatched patients were significantly lower than those in peripheral and control areas. The MK and MD maps showed a lesion area of 20.08 ± 5.74 cm² and 22.09 ± 5.58 cm², respectively. T2WI showed a lesion area of 19.76 ± 5.02 cm². There were no significant differences in the cerebral infarction lesion areas measured using the three methods. MK, MD, and T2WI showed a good correlation.

CONCLUSION

DKI parameters showed significant difference between the focal and control areas in patients with acute ischemic cerebral infarction. 3DASL can effectively determine the changes in perfusion levels in the lesion area. There was a high correlation between the area of the infarct lesions diagnosed by DKI and T2WI.

Key Words: Magnetic resonance; Multi-delay 3D arterial spin labeling; Diffusion kurtosis imaging; Acute ischemic cerebral infarction; Perfusion; Nerve function

©The Author(s) 2022. Published by Baishideng Publishing Group Inc. All rights reserved.

Core Tip: Through the analysis and research of patients in the hospital, we have concluded that diffusion kurtosis imaging (DKI) parameters show that there is a significant difference between the lesions of patients with acute ischemic cerebral infarction and the control area. Three-dimensional arterial spin labeling can effectively determine the changes in the perfusion level of the diseased area. The infarct size diagnosed by DKI is highly correlated with T2-weighted imaging.

Citation: Jiang YY, Zhong ZL, Zuo M. Three-dimensional arterial spin labeling and diffusion kurtosis imaging in evaluating perfusion and infarct area size in acute cerebral ischemia. *World J Clin Cases* 2022; 10(17): 5586-5594

URL: <https://www.wjgnet.com/2307-8960/full/v10/i17/5586.htm>

DOI: <https://dx.doi.org/10.12998/wjcc.v10.i17.5586>

INTRODUCTION

Cerebral infarction mainly occurs in geriatric patients, and it is a common clinical cerebrovascular disease with high disability and fatality rates. Therefore, it can severely affect patients' quality of life and health. Clinical practice has demonstrated that early and effective thrombolytic therapy can significantly improve the prognosis of patients with acute cerebral infarction, and that treatment options vary according to the severity of the infarction[1]. Therefore, it is important to explore effective methods for the accurate diagnosis of cerebral infarction to improve the treatment modalities and prognosis.

Magnetic resonance imaging (MRI) has important advantages in the diagnosis of central nervous system diseases due to its high soft tissue resolution. Multi-delay three-dimensional arterial spin labeling (3DASL) can accurately evaluate cerebral blood flow (CBF). Diffusion kurtosis imaging (DKI) is a clinical imaging method used to describe the non-Gaussian diffusion of water molecules in tissues; it can accurately reflect the complexity and heterogeneity of neural tissue microstructure by quantifying the diffusion characteristics of water molecules[2,3]. Our study aimed to investigate the diagnostic value of magnetic resonance multi-delay 3DASL and DKI in evaluating the perfusion and infarct area size in patients with acute cerebral ischemia.

MATERIALS AND METHODS

Baseline data

A total of 84 patients who experienced acute cerebral ischemia from March 2019 to February 2021 in our hospital were selected. The inclusion criteria were as follows: Patients (1) Aged 57–82 years; (2) diagnosed with unilateral acute ischemic cerebral infarction (diagnostic criteria of the Fourth National Academic Conference on Cerebrovascular Diseases in 1996)[4]; (3) with dizziness, vomiting, limb numbness, and headache as the main clinical manifestations; (4) who were hospitalized within 24 h of the onset of the disease and who underwent MRI; and (5) who provided informed consent before the relevant examination. The exclusion criteria were as follows: Patients with (1) Cerebrovascular hemorrhagic diseases (hypertensive cerebral hemorrhage, aneurysm, arterial malformation); (2) intracranial tumors; (3) a history of craniotomy; (4) a history of acute myocardial infarction and had an implanted pacemaker placed less than 3 mo previously; (5) cochlear implants and other such complications; (6) mental illness and hyperthyroidism; and (7) a history of drug allergy. The study tender and related materials was implemented after the decision of the medical ethics committee.

MRI and data collection

A 3DASL scan was performed using our MRI scanner (1.5 T, 8-channel cranial coil) from the cranial top to the lower margin of the foramen magnum. Conventional transverse T1-weighted imaging, T2-weighted imaging (T2WI), and coronal fat-suppressed (FS) + fluid-attenuated inversion recovery imaging were performed. The 3DASL sequence adopted 3D spiral fast spin echo technology. The scanning parameters were as follows: echo time (TE), 10.5 ms; repetition time (TR), 4548 ms; labeling delay time, 1.5; layer thickness, 4 mm; and post-labeling delay (PLD), 1525. The CBF values of PLD1.5s and PLD2.5s were obtained.

The DKI sequence scanning parameters were as follows: TR, 6000 ms; layer thickness, 5 mm; TE, minimum; layer spacing, 1.5 mm; field of vision, 240 mm × 240 mm; matrix, 96 × 130; diffusion direction, 15; and B = 0, 1000, and 2000 s/mm². The images obtained were analyzed by the supporting software for the following DKI parameters: apparent diffusion coefficient (ADC), axial tensor (AD), mean diffusion coefficient (MD), radial tensor (RD), mean kurtosis (MK), radial kurtosis (RK), and axial kurtosis (AK).

Image and data processing

The original data were processed using a GEMR processing workstation. Two imaging physicians with a senior professional title in our hospital agreed to select the infarction area, abnormal ASL perfusion area, mismatching area, and corresponding contralateral normal brain tissue as regions of interest (ROIs). The CBF value of each ROI area and the ADC value were measured and calculated.

Statistical analysis

In this study, the DKI parameters, CBF values under PLD1.5s and PLD2.5s, and other measurement indices were consistent with the approximate normal distribution or the normal distribution by a normal distribution test, and they are expressed as mean ± SD. The *t*-test was used for group comparisons. The Statistical Package for the Social Sciences (version 21.0; IBM, Armonk, NY) was used for data analysis. The inspection level was $\alpha = 0.05$.

RESULTS

Comparison of baseline data between the joint and control groups

The age, body mass index, and time from onset to admission of the study subjects were 57–82 (average, 68.8 ± 5.8) years, 23.8 ± 2.1 kg/m², and 9–24 (average, 14.2 ± 4.0) h, respectively. The study subjects included 48 males and 36 females. A total of 27 and 30 patients smoked and consumed alcohol, respectively. Moreover, 29, 15, 16, and 34 patients had hypertension, diabetes, coronary heart disease, and hyperlipidemia, respectively. The National Institutes of Health Stroke Scale (NIHSS) score within 24 h after admission ranged from 11–18 points, and the average NIHSS score was 14.8 ± 2.2 points.

Comparison of DKI parameters between the lesion and control areas

The DKI parameters of the focal and control areas in the study subjects were compared. The ADC, MD, AD, and RD values in the lesion area were significantly lower than those in the control areas ($P < 0.05$). The MK, RK, and AK values in the lesion area were significantly higher than those in the control area ($P < 0.05$) (Table 1).

Comparison of perfusion parameters between the lesion and control areas under different PLDs

The CBF values of the focal area of the study subjects at PLD1.5s and PLD2.5s were significantly lower than that of the control area ($P < 0.05$). The results are presented in Table 2 and Figure 1.

Table 1 Comparison of diffusion kurtosis imaging parameters between the lesion and control areas (mean ± SD)

Indexes	The lesion area (n = 84)	The control area (n = 84)	t value	P value
ADC	576.3 ± 94.2	756.0 ± 102.1	-11.856	0.000
MD	0.651 ± 0.150	0.847 ± 0.167	-8.003	0.000
AD	0.830 ± 0.167	1.305 ± 0.204	-16.513	0.000
RD	0.531 ± 0.093	0.644 ± 0.122	-6.751	0.000
AK	1.281 ± 0.224	0.760 ± 0.115	18.964	0.000
MK	1.256 ± 0.241	0.922 ± 0.207	9.636	0.000
RK	1.328 ± 0.304	0.987 ± 0.185	8.782	0.000

ADC: Apparent diffusion coefficient; MD: Average diffusion coefficient; AD: Axial diffusion; RD: Radial diffusion; AK: Axial kurtosis; MK: Average kurtosis; RK: Radial kurtosis.

Table 2 Comparison of cerebral blood flow values between the lesion area and control area under different parameters of different delay time after labeling (mean ± SD, mL/100 g/min)

Groups	n	PLD1.5s	PLD2.5s
Focal area	84	22.64 ± 5.81	14.03 ± 3.91
Control area	84	34.51 ± 7.03	37.58 ± 7.76
t value		-11.929	-24.839
P value		0.000	0.000

PLD: Perfusion parameters post-labeling delays.

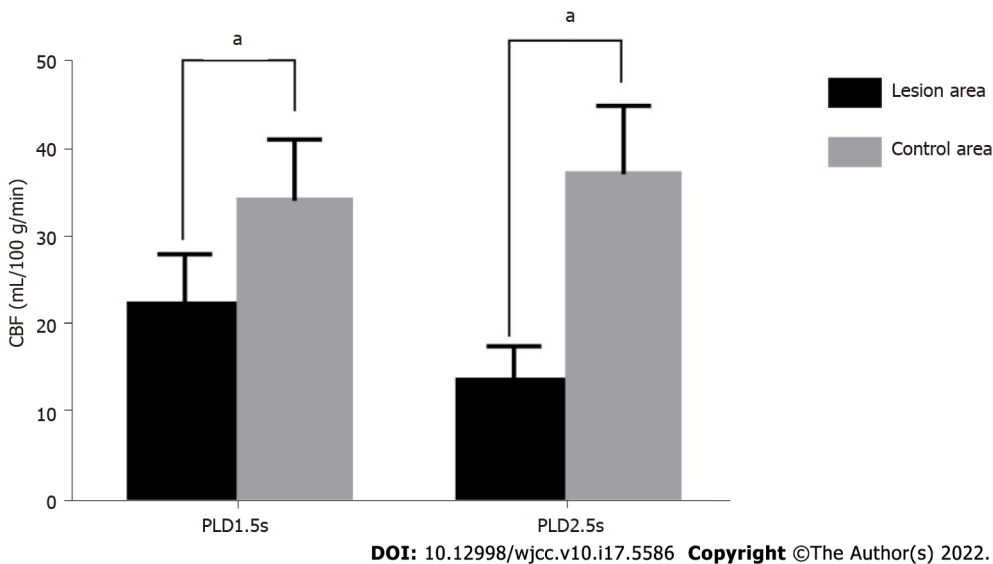


Figure 1 Histogram of cerebral blood flow values of the lesion and control areas under parameters of different delay time after labeling 1.5 s and 2.5 s. ^aP < 0.05 vs control areas. CBF: Cerebral blood flow; PLD: Parameters of different delay time.

Comparison of PLD1.5s perfusion parameters of MK/MD-matched and -unmatched infarct lesions

The MK/MD value in the infarct lesions was used to determine the matching situation. MK/MD < 5 mm was considered matching, whereas MK/MD ≥ 5 mm was considered mismatching. The PLD1.5s perfusion parameters in the central, peripheral, and control areas of the infarct lesions in MK/MD-matched and -unmatched patients were not significantly different (P > 0.05). The PLD1.5s perfusion parameter values in the central area of infarct lesions in MK/MD-matched and -unmatched lesions were significantly lower than those in peripheral and control areas (P < 0.05) (Table 3).

Table 3 Comparison of parameters of different delay time after labeling 1.5s perfusion parameters of average kurtosis/average diffusion coefficient-matched and unmatched infarct lesions (mean ± SD, mL/100 g/min)

Lesion area	MK/MD unmatched (n = 48)	MK/MD matched (n = 36)	t value	P value
Central are	16.33 ± 4.75	17.50 ± 4.82	-1.110	0.270
Peripheral area	26.95 ± 5.30 ^{a,d}	28.03 ± 5.47 ^{a,d}	-0.912	0.365
Unmatched area	25.73 ± 5.54 ^{a,d}	-		
Matched area	34.60 ± 6.95 ^d	34.12 ± 6.85 ^d	0.315	0.753
F value	29.064	28.551		
P value	0.000	0.000		

^aP < 0.05 vs the control area.

^dP < 0.05 vs the central area.

MK: Average kurtosis; MD: Average diffusion coefficient.

Comparison of PLD2.5s perfusion parameters of MK/MD-matched and -unmatched infarct lesions

The PLD2.5s perfusion parameters in the central, peripheral, and control areas of the infarct lesions in MK/MD-matched and -unmatched patients were not significantly different (P > 0.05). The values of the PLD2.5s perfusion parameters in the central area of infarct lesions in MK/MD-matched and -unmatched patients were significantly lower than those in peripheral and control areas (P < 0.05) (Table 4).

Results of low perfusion area measurement

The MK map showed an infarct area of 20.08 ± 5.74 cm², and the MD map showed an area of 22.09 ± 5.58 cm² in the study subjects. T2WI showed a lesion area of 19.76 ± 5.02 cm². There were no significant differences in the cerebral infarction areas measured using these three methods (F = 2.094, P = 0.227). MK, MD, and T2WI showed a good correlation (r = 0.617, r = 0.620, P < 0.05) (Figure 2A and B).

Case introduction

A 67-year-old male patient was admitted to the hospital due to dizziness, vomiting, and limb dysfunction for 12 h (Figure 3).

DISCUSSION

The traditional method used for clinical diagnosis of cerebral infarction relies on computed tomography (CT), which evaluates the absorption of different types of radiation by different tissues. However, some studies[5-7] have suggested that CT diagnosis and evaluation of cerebral infarction often cannot be performed within 6 h of onset, thus affecting the treatment.

DKI technology analyzes the motion of water molecules in tissues in a non-Gaussian distribution, which is closer to the real motion characteristics of water molecules, and is an extension of magnetic resonance diffusion tensor imaging and magnetic resonance diffusion-weighted imaging[8,9]. In our study, the ADC, MD, AD, and RD values in the lesion area were significantly lower than those in the control group, whereas the MK, RK, and AK values were significantly higher than those in the control group. DKI was more prone to uneven signals due to the large variation in DKI parameters when taken soon after the cerebral infarction occurred, suggesting that DKI has a higher sensitivity in differentiating ischemic brain injuries and can be used as an indicator of complexity and heterogeneity of the changes in the microenvironment inside the cerebral infarction tissue. The movement of water molecules in brain tissue is restricted by the cell membrane, organelles, axons, and myelin sheath; therefore, water molecules in brain tissue cannot show the ideal normal distribution diffusion movement because of restricted movement. Therefore, DKI is more sensitive to pathological changes in brain tissue after ischemia than DWI and DTI, and it is conducive for a more comprehensive analysis of the micro-structural changes in cerebral infarction[10-12].

3DASL technology is a type of perfusion imaging with total brain volume coverage and can be used to determine the appropriate treatment method for stroke. In this study, the CBF values of the focal area in the study subjects at PLD1.5s and PLD2.5s were significantly lower than that of the control area. 3DASL is a non-invasive and quantitative diagnostic method, which can accurately evaluate blood flow in the entire brain, determine the blood flow status of the local infarction area, quantitatively analyze blood flow velocity, and evaluate the establishment of collateral circulation, which is of crucial significance for the formulation of a treatment plan and the evaluation of its curative effect[13-15].

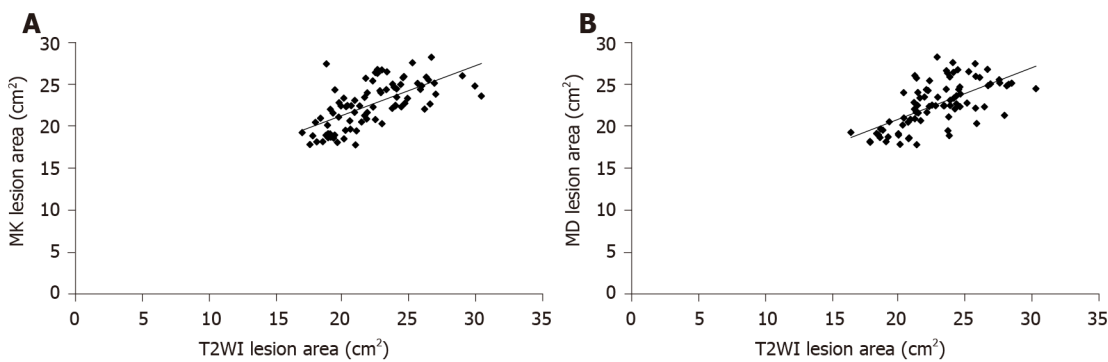
Table 4 Comparison of parameters of different delay time after labeling 2.5s perfusion parameters of average kurtosis/average diffusion coefficient-matched and unmatched infarct lesions (mean ± SD, mL/100 g/min)

Lesion area	MK/MD unmatched (n = 48)	MK/MD matched (n = 36)	t value	P value
Central area	11.50 ± 3.89	12.28 ± 4.03	-0.896	0.373
Peripheral area	25.84 ± 6.03 ^{a,d}	26.71 ± 5.94 ^{a,d}	-0.659	0.512
Unmatched area	21.76 ± 5.20 ^{a,d}	-	-	-
Control area	37.85 ± 7.54	38.90 ± 7.41 ^d	-0.636	0.526
F value	41.025	43.008		
P value	0.000	0.000		

^aP < 0.05 vs the control area.

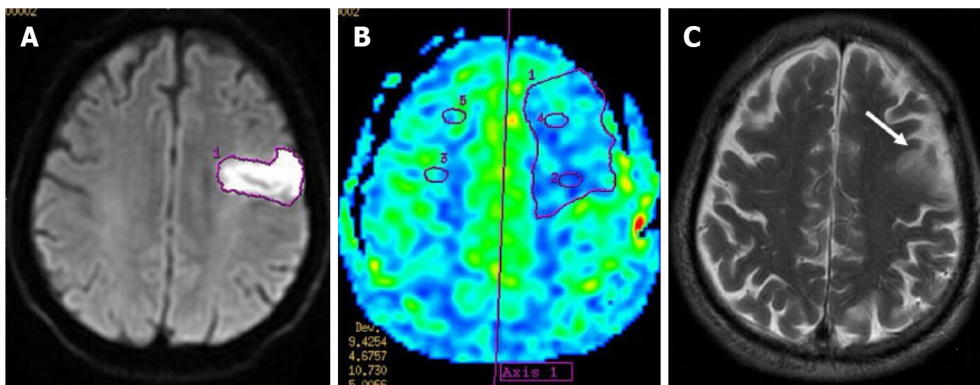
^dP < 0.05 vs the central area.

MK: Average kurtosis; MD: Average diffusion coefficient.



DOI: 10.12998/wjcc.v10.i17.5586 Copyright ©The Author(s) 2022.

Figure 2 Correlation between the average kurtosis, the average diffusion coefficient, and the area of cerebral infarction on T2-weighted imaging. A: Correlation between the average kurtosis and the area of cerebral infarction; B: Correlation between the average diffusion coefficient and the area of cerebral infarction. MD: Average diffusion coefficient; MK: Average kurtosis; T2WI: T2-weighted imaging.



DOI: 10.12998/wjcc.v10.i17.5586 Copyright ©The Author(s) 2022.

Figure 3 A 67-year-old male patient was admitted to the hospital due to dizziness, vomiting, and limb dysfunction for 12 h. Magnetic resonance imaging examination was performed within 4 h after admission, and the patient was diagnosed with acute cerebral infarction in the left frontal lobe. A: The diffusion-weighted imaging image and the focal area of cerebral infarction showing high signal performance; B: The color map of cerebral perfusion, showing significant hypoperfusion in the infarct lesion area; C: T2-weighted imaging, with the infarct area indicated by the white arrow showing high signal intensity (Arrow).

The comparison of the PLD1.5s and PLD2.5s perfusion parameters between the two groups showed that the values of the PLD1.5s perfusion parameters in the central area of infarct lesions in MK/MD-matched and -unmatched patients were significantly lower than those in the peripheral and control areas. 3DASL, as a whole-brain non-invasive volume perfusion evaluation technology, can provide quantitative and accurate whole-brain blood perfusion information and help in the precise and early

diagnosis and treatment of stroke. Moreover, the selection of the PLD is important for the analysis of ASL results. PLD1.5s showed the perfusion behavior and the compensatory ability of rapid collateral circulation and PLD2.5s showed the perfusion result. The results of this study also suggested that 3DASL can effectively evaluate and determine the infarct area[16].

The results of the low perfusion area measurement indicated that MK, MD, and T2WI showed no significant differences in the measurement of the area of cerebral infarction lesions in the study subjects, suggesting that these three modalities showed good correlation. The MK and MD values are dependent on the complexity of the tissue microstructure in the ROI and are the most representative parameters of DKI, which can show the degree of limited diffusion of water molecules and the complexity of tissue microstructure. The more complex the structure, the more evident the limited diffusion of water molecules and the larger the MK and MD values[17-20]; whereas there was a significant increase in CBF value on T2WI of the cerebral infarction area, which was closely correlated with MK, MD, and T2WI.

CONCLUSION

In conclusion, the difference in DKI parameters between the focal and control areas in patients with acute ischemic cerebral infarction is significant, which is important for the diagnosis of infarction. 3DASL can effectively determine the changes in perfusion levels in the lesion area. There was a high correlation between the area of the infarct lesions diagnosed by DKI and T2WI.

ARTICLE HIGHLIGHTS

Research background

Early thrombolytic therapy is crucial to treat acute cerebral infarction, especially since the onset of thrombolytic therapy takes 1–6 h. Therefore, early diagnosis and evaluation of cerebral infarction is important.

Research motivation

This study explored the methods for assessing perfusion and infarct size in patients with acute cerebral ischemia.

Research objectives

The study aimed to investigate the diagnostic value of magnetic resonance multi-delay three-dimensional arterial spin labeling (3DASL) and diffusion kurtosis imaging (DKI) in evaluating the perfusion and infarct area size in acute cerebral ischemia patients.

Research methods

Eighty-four patients who experienced acute cerebral ischemia from March 2019 to February 2021 were included.

Research results

The apparent diffusion coefficient, average diffusion coefficient (MD), axial diffusion, and radial diffusion values in the lesion area were significantly lower than those in the control area. The average kurtosis (MK), radial kurtosis, and axial kurtosis values in the lesion area were significantly higher than those in the control area. parameters post-labeling delays (PLD) 1.5s and PLD2.5s perfusion parameters in the central, peripheral, and control areas of the infarct lesions in MK/MD-matched and -unmatched patients were not significantly different. PLD1.5s and PLD2.5s perfusion parameter values in the central area of the infarct lesions in MK/MD-matched and -unmatched patients were significantly lower than those in peripheral and control areas. There were no significant differences in the cerebral infarction lesion areas measured using the three methods.

Research conclusions

DKI parameters showed significant difference between the focal and control areas in patients with acute ischemic cerebral infarction. 3DASL can effectively determine the changes in perfusion levels in the lesion area. There was a high correlation between the area of the infarct lesions diagnosed by DKI and T2-weighted imaging.

Research perspectives

3DASL and DKI have broader application value in assessing perfusion and infarct size in patients with acute cerebral ischemia.

FOOTNOTES

Author contributions: Jiang YY and Zhong ZL contributed equally to this study, and should be regarded as co-first authors, Jiang YY and Zhong ZL designed the study and collected the data; Zuo M drafted the manuscript, Zuo M and Jiang YY analyzed and interpreted data.

Institutional review board statement: This study was approved by the Wuhan Yaxin General Hospital Ethics Committee.

Informed consent statement: All study participants, or their legal guardian, provided informed written consent prior to study enrollment.

Conflict-of-interest statement: The authors declare that there are no conflicts of interest.

Data sharing statement: No additional data are available.

Open-Access: This article is an open-access article that was selected by an in-house editor and fully peer-reviewed by external reviewers. It is distributed in accordance with the Creative Commons Attribution NonCommercial (CC BY-NC 4.0) license, which permits others to distribute, remix, adapt, build upon this work non-commercially, and license their derivative works on different terms, provided the original work is properly cited and the use is non-commercial. See: <https://creativecommons.org/licenses/by-nc/4.0/>

Country/Territory of origin: China

ORCID number: Yan-Yan Jiang 0000-0001-7831-6775; Zhi-Lin Zhong 0000-0002-9215-3578; Min Zuo 0000-0001-7205-1462.

S-Editor: Wang JL

L-Editor: A

P-Editor: Wang JL

REFERENCES

- 1 **Zhu LH**, Zhang ZP, Wang FN, Cheng QH, Guo G. Diffusion kurtosis imaging of microstructural changes in brain tissue affected by acute ischemic stroke in different locations. *Neural Regen Res* 2019; **14**: 272-279 [PMID: 30531010 DOI: 10.4103/1673-5374.244791]
- 2 **Yang Z**, Rong Y, Cao Z, Wu Y, Zhao X, Xie Q, Luo M, Liu Y. Microstructural and Cerebral Blood Flow Abnormalities in Subjective Cognitive Decline Plus: Diffusional Kurtosis Imaging and Three-Dimensional Arterial Spin Labeling Study. *Front Aging Neurosci* 2021; **13**: 625843 [PMID: 33597860 DOI: 10.3389/fnagi.2021.625843]
- 3 **Mao C**, Fu Y, Ye X, Wu A, Yan Z. [Study of 3D-pcASL in differentiation of acute cerebral infarction and acute encephalitis]. *Zhonghua Yi Xue Za Zhi* 2015; **95**: 1846-1848 [PMID: 26712404]
- 4 **Frank L**, Burigk L, Lehmsbecker A, Wohlsein P, Schütter A, Meyerhoff N, Tipold A, Nessler J. Meningioma and associated cerebral infarction in three dogs. *BMC Vet Res* 2020; **16**: 177 [PMID: 32503537 DOI: 10.1186/s12917-020-02388-2]
- 5 **Kong LM**, Zeng JY, Zheng WB, Shen ZW, Wu RH. Effects of Acute Alcohol Consumption on the Human Brain: Diffusional Kurtosis Imaging and Arterial Spin-Labeling Study. *AJNR Am J Neuroradiol* 2019; **40**: 641-647 [PMID: 30872417 DOI: 10.3174/ajnr.A5992]
- 6 **Zhou IY**, Guo Y, Igarashi T, Wang Y, Mandeville E, Chan ST, Wen L, Vangel M, Lo EH, Ji X, Sun PZ. Fast diffusion kurtosis imaging (DKI) with Inherent CORrelation-based Normalization (ICON) enhances automatic segmentation of heterogeneous diffusion MRI lesion in acute stroke. *NMR Biomed* 2016; **29**: 1670-1677 [PMID: 27696558 DOI: 10.1002/nbm.3617]
- 7 **Sun PZ**, Wang Y, Mandeville E, Chan ST, Lo EH, Ji X. Validation of fast diffusion kurtosis MRI for imaging acute ischemia in a rodent model of stroke. *NMR Biomed* 2014; **27**: 1413-1418 [PMID: 25208309 DOI: 10.1002/nbm.3188]
- 8 **Lu D**, Jiang Y, Ji Y, Zhou IY, Mandeville E, Lo EH, Wang X, Sun PZ. JOURNAL CLUB: Evaluation of Diffusion Kurtosis Imaging of Stroke Lesion With Hemodynamic and Metabolic MRI in a Rodent Model of Acute Stroke. *AJR Am J Roentgenol* 2018; **210**: 720-727 [PMID: 29470156 DOI: 10.2214/AJR.17.19134]
- 9 **Arab A**, Ruda-Kucerova J, Minsterova A, Drazanova E, Szabó N, Starcuk Z Jr, Rektorova I, Khairnar A. Diffusion Kurtosis Imaging Detects Microstructural Changes in a Methamphetamine-Induced Mouse Model of Parkinson's Disease. *Neurotox Res* 2019; **36**: 724-735 [PMID: 31209787 DOI: 10.1007/s12640-019-00068-0]
- 10 **Tan ZR**, Zhang C, Tian FF. Spectrum of clinical features and neuroimaging findings in acute cerebral infarction patients with unusual ipsilateral motor impairment- a series of 22 cases. *BMC Neurol* 2019; **19**: 279 [PMID: 31718589 DOI: 10.1186/s12883-019-1516-y]
- 11 **Suman G**, Rusin JA, Lebel RM, Hu HH. Multidelay Arterial Spin Labeling MRI in the Assessment of Cerebral Blood Flow: Preliminary Clinical Experience in Pediatrics. *Pediatr Neurol* 2020; **103**: 79-83 [PMID: 31570299 DOI: 10.1016/j.pediatrneurol.2019.08.005]
- 12 **Qu Y**, Zhou L, Jiang J, Quan G, Wei X. Combination of three-dimensional arterial spin labeling and stretched-exponential model in grading of gliomas. *Medicine (Baltimore)* 2019; **98**: e16012 [PMID: 31232933 DOI: 10.1097/MD.00000000000016012]

- 13 **Tortora D**, Severino M, Rossi A. Arterial spin labeling perfusion in neonates. *Semin Fetal Neonatal Med* 2020; **25**: 101130 [PMID: [32591228](#) DOI: [10.1016/j.siny.2020.101130](#)]
- 14 **Uetani H**, Kitajima M, Sugahara T, Muto Y, Hirai K, Kuroki Y, Nakaura T, Tateishi M, Yamashita Y. Perfusion abnormality on three-dimensional arterial spin labeling in patients with acute encephalopathy with biphasic seizures and late reduced diffusion. *J Neurol Sci* 2020; **408**: 116558 [PMID: [31715327](#) DOI: [10.1016/j.jns.2019.116558](#)]
- 15 **Aoike S**, Sugimori H, Fujima N, Suzuki Y, Shimizu Y, Suwa A, Ishizaka K, Kudo K. Three-dimensional Pseudo-continuous Arterial Spin-labeling Using Turbo-spin Echo with Pseudo-steady State Readout: A Comparison with Other Major Readout Methods. *Magn Reson Med Sci* 2019; **18**: 170-177 [PMID: [30318501](#) DOI: [10.2463/mrms.tn.2018-0031](#)]
- 16 **Shinohara Y**, Kato A, Kuya K, Okuda K, Sakamoto M, Kowa H, Ogawa T. Perfusion MR Imaging Using a 3D Pulsed Continuous Arterial Spin-Labeling Method for Acute Cerebral Infarction Classified as Branch Atheromatous Disease Involving the Lenticulostriate Artery Territory. *AJNR Am J Neuroradiol* 2017; **38**: 1550-1554 [PMID: [28596191](#) DOI: [10.3174/ajnr.A5247](#)]
- 17 **Wei Y**, Wu L, Wang Y, Liu J, Miao P, Wang K, Wang C, Cheng J. Disrupted Regional Cerebral Blood Flow and Functional Connectivity in Pontine Infarction: A Longitudinal MRI Study. *Front Aging Neurosci* 2020; **12**: 577899 [PMID: [33328960](#) DOI: [10.3389/fnagi.2020.577899](#)]
- 18 **Wang C**, Miao P, Liu J, Wei S, Guo Y, Li Z, Zheng D, Cheng J. Cerebral blood flow features in chronic subcortical stroke: Lesion location-dependent study. *Brain Res* 2019; **1706**: 177-183 [PMID: [30419222](#) DOI: [10.1016/j.brainres.2018.11.009](#)]
- 19 **Lin L**, Chen X, Jiang R, Zhong T, Du X, Xu G, Duan Q, Xue Y. Differentiation between vestibular schwannomas and meningiomas with atypical appearance using diffusion kurtosis imaging and three-dimensional arterial spin labeling imaging. *Eur J Radiol* 2018; **109**: 13-18 [PMID: [30527294](#) DOI: [10.1016/j.ejrad.2018.10.009](#)]
- 20 **Hoehn M**, Küstermann E, Blunk J, Wiedermann D, Trapp T, Wecker S, Föcking M, Arnold H, Hescheler J, Fleischmann BK, Schwandt W, Bührle C. Monitoring of implanted stem cell migration in vivo: a highly resolved *in vivo* magnetic resonance imaging investigation of experimental stroke in rat. *Proc Natl Acad Sci U S A* 2002; **99**: 16267-16272 [PMID: [12444255](#) DOI: [10.1073/pnas.242435499](#)]



Published by **Baishideng Publishing Group Inc**
7041 Koll Center Parkway, Suite 160, Pleasanton, CA 94566, USA
Telephone: +1-925-3991568
E-mail: bpgoffice@wjgnet.com
Help Desk: <https://www.f6publishing.com/helpdesk>
<https://www.wjgnet.com>

